Electrochimica Acta 55 (2010) 5561–5568

Contents lists available at ScienceDirect

Electrochimica Acta

journal homepage: www.elsevier.com/locate/electacta

Mechanism of glucose electrochemical oxidation on gold surface

Mauro Pasta[a,b], Fabio La Mantia[b,1], Yi Cui[b,*]

[a] Dipartimento di Chimica Inorganica, Metallorganica e Analitica "Lamberto Malatesta", Università degli Studi di Milano, Via Venezian 21, 20133 Milano, Italy
[b] Department of Material Science and Engineering, Stanford University, 476 Lomita Mall, Stanford, CA 94305, United States

ARTICLE INFO

Article history:
Received 2 March 2010
Received in revised form 12 April 2010
Accepted 18 April 2010
Available online 24 April 2010

Keywords:
Glucose electrochemical oxidation
Glucose sensing
Gold electrochemical oxidation
Reaction mechanism
Electrochemical impedance spectroscopy

ABSTRACT

The complex oxidation of glucose at the surface of gold electrodes was studied in detail in different conditions of pH, buffer and halide concentration. As observed in previous studies, an oxidative current peak occurs during the cathodic sweep showing a highly linear dependence on glucose concentration, when other electrolyte conditions are unchanged. The effect of the different conditions on the intensity of this peak has stressed the limitations of the previously proposed mechanisms. A mechanism able to explain the presence of this oxidative peak was proposed. The mechanism takes into account ion-sorption and electrochemical adsorption of OH^-, buffer species (K_2HPO_4/KH_2PO_4) and halides.

1. Introduction

Electrochemical oxidation of glucose has generated much interest over the years. It has been extensively studied for applications in glucose–oxygen fuel cells [1] and, especially, in glucose sensors, [2] whose optimization (in terms of response time, lifetime, sensitivity and selectivity) is required to improve the treatment of diabetes mellitus, a chronic disease affecting millions of people around the world [3].

The electrocatalytic oxidation of glucose in alkaline medium was investigated using Cu, Ni, Fe, Pt and Au electrodes [4]. Among them, platinum has been the most widely studied [5–9]; in particular Beden et al. applied a reflectance IR spectroscopic technique to study the electro-oxidation process of D-glucose at platinum electrodes in alkaline medium [10]. However, platinum also proved to be extremely non-selective and susceptible to poisoning by various components of blood and other physiological media over extended use [9,11,12].

Gold is an attractive metal for the oxidation of glucose, because its oxidation potential in neutral and alkaline medium is more negative compared to the other metals [13,14] and therefore has been extensively examined [4,14–23].

Nikolaeva et al. proposed a mechanism for glucose electrooxidation at high potentials, in which a layer of gold oxide formed on the surface of a gold electrode could have a great catalytic effect on glucose oxidation [24]. The suggested mechanism was the following:

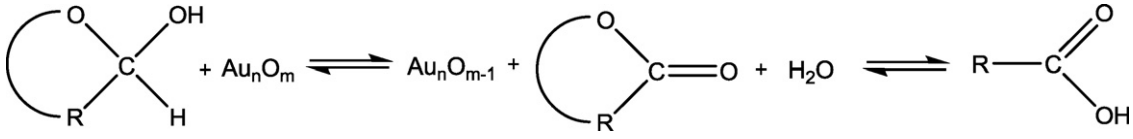

or

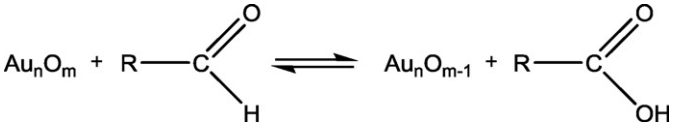

This reaction was followed by rapid electrochemical regeneration of the surface oxide

$$Au_nO_{m-1} + 2OH^- \rightleftharpoons Au_nO_m + H_2O + 2e^-$$

In a subsequent study, Makovos and Liu first identified a positive current peak during the cathodic sweep in cyclic voltammetry and highlighted a highly linear dependence between the maxima of current values and glucose concentration in a wide potential range depending on the medium composition [25]. They also proposed

* Corresponding author. Tel.: +1 6507234613; fax: +1 6507254034.
E-mail address: yicui@stanford.edu (Y. Cui).
[1] ISE member.

0013-4686/$ – see front matter © 2010 Published by Elsevier Ltd.
doi:10.1016/j.electacta.2010.04.069

a different mechanism for the peak generation, claiming that the one provided by Nikolaeva et al. did not account for the fact that the reaction proceeds only when the potential favors a partial reduction of the gold oxide:

$$Au_nO_m + 2e^- \rightleftharpoons Au_nO_{m-1} + O^{2-}$$

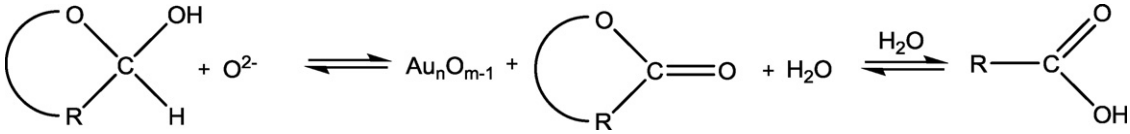

Followed by:

$$Au_nO_{m-1} + 2OH^- \rightleftharpoons Au_nO_m + H_2O + 2e^-$$

Chlorides, amino acids, and human albumin were observed to inhibit the reaction whereas urea and L-ascorbic acid contributed a stabilizing effect to the performance of the electrode. They concluded that gold oxide might be successfully utilized as catalyst for glucose oxidation in a glucose sensor or a biological fuel cell, if a proper separation of the inhibitors was achieved. In fact, this is the basis of the pulsed amperometric detection technique (PAD) at gold electrodes which, coupled with liquid chromatography (LC), gained prominence for the analysis of complex mixtures of polyalcohols and carbohydrates in alkaline medium [26].

Nevertheless the presence of the previously reported inhibitors forbids the direct application of this system in blood, where it is mainly required. Among these inhibiting species, chlorides are the most problematic because they are present in a high concentration in the blood (about 0.1 M) and their separation from glucose is difficult to achieve.

Makovos and Liu attempted to use a gold electrode in media containing chloride ions, but discovered that chloride ions, even at trace levels, strongly inhibit any response toward glucose.

They suggested that the presence of Cl^- ions caused gold to dissolve instead of forming an oxide layer:

$$Au + 4Cl^- \rightarrow AuCl_4^- + 3e^-$$

Consequently, the unoxidized gold has no electrocatalytic activity with respect to the oxidation of glucose.

Many questions remain unanswered by the mechanisms proposed by Nikoleava and Makovos:

(1) If these mechanisms are correct, the charge under the cathodic oxidative peak current should show a dependence on the oxide thickness, not on the glucose concentration.
(2) The last step proposed in both mechanisms is gold re-oxidation, however it is difficult to imagine this re-oxidation taking place at such a low potential (down to 0.0 V vs. RHE) when the same reaction (initial formation of the oxide) in the anodic sweep starts at 0.8 V vs. RHE.
(3) The peak onset is very sharp, but there is also a long tail after the main peak which is difficult to explain with the proposed mechanism: instead it seems that the reduction of the oxide enables the oxidation of the glucose.
(4) The data does not conclusively suggest that gold oxide is really what is formed in these conditions.

In the present study we investigated the effects of varying chloride concentration, pH and buffer conditions on the electrooxidation of glucose at a gold electrode, proposing a mechanism for the positive current peak formation during the cathodic sweep. The comprehension of the mechanisms behind the formation of this peak was necessary to the authors to correctly lay the groundwork for upcoming work concerning glucose sensing.

2. Experimental

D(+)-Glucose (dextrose) anhydrous, potassium chloride, sodium fluoride, PBS (phosphate buffer solution: 100 mM NaCl, 10 mM KCl, 10 mM KH_2PO_4 and 10 mM K_2HPO_4), potassium phosphate dibasic and potassium phosphate monobasic were purchased from Sigma Aldrich. A gold pin electrode (surface area 0.0314 cm^2) and a platinum counter electrode were purchased from Amel Electrochemistry.

Electrochemical characterization was carried out using a Bio-Logic VMP3 potentiostat–galvanostat multichannel equipped with EIS board. A double junction Ag|AgCl|KCl (3.5 M) reference electrode (RE) was used in the measurement. The double junction was employed to prevent OH^- diffusion and reaction at the Ag/AgCl interface; additionally, the RE potential was monitored after each measurement to confirm that no change had taken place. Before each measurement, the gold pin electrode surface was activated and stabilized in 0.1 M KOH by CV scans at 100 mV s^{-1} between −0.7 and 0.8 V vs. RE until stable voltammograms were observed (about 20 scans). All the measurements were performed under inert (nitrogen) atmosphere and room temperature.

3. Results and discussion

Fig. 1 shows a typical cyclic voltammogram of glucose electrooxidation in alkaline solution. The discussion of the overall mechanism is not the aim of this work; a deep analysis has been already discussed by Beden et al. at platinum electrodes and low temperature [10]. The aim of the present work is to understand the influence of different species in the electrolyte on the generation of peak (*) in Fig. 1.

The Pourbaix diagram of Au in aqueous solutions (see Fig. 2) stresses that in the pH range 7–12, gold is oxidized to Au(III) hydroxide, the oxidation potential decreasing as the pH is increased. Above pH 12.5, gold is oxidized to the water-soluble ion $HAuO_3^{2-}$.

According to the diagram, cyclic voltammetry measurements performed at a gold pin working electrode in a 100 mM

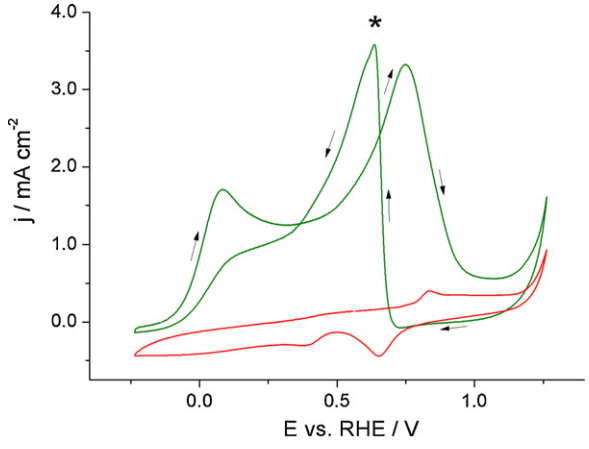

Fig. 1. Cyclic voltammetry of a gold pin electrode in 0.1 M KOH without (red curve) and with (green curve) 10 mM glucose; scan rate 100 mV s^{-1}. (For interpretation of the references to colors in this figure legend, the reader is referred to the web version of this article.)

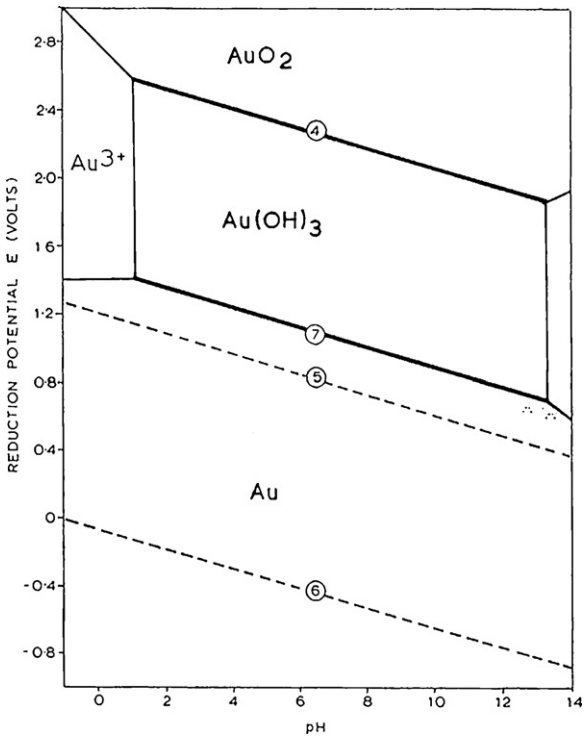

Fig. 2. Pourbaix diagram for the system Au–H_2O at 25 °C. The concentration of all the soluble species is 10^{-4} M. Extract from Ref. [29].

K_2HPO_4–KH_2PO_4 solution without glucose at different pH values (see Fig. 3) show a peak relative to the formation of the gold hydroxide (around 1 V vs. RHE), which is successively reduced in the negative sweep (0.75 V vs. RHE). Two other peaks, one in the oxidative (0.55 V vs. RHE) and the other in the reductive scan (0.5 V vs. RHE) (both clearly visible at pH 11.5), have been attributed to the chemisorption of the hydroxide ion to the Au surface [27].

When glucose (10 mM) is added to the electrolyte (Fig. 4) the oxidative peak (*) appears. Its current density depends strongly on the pH of the solution.

Fig. 5 shows the Pourbaix diagram of Au in a 2 M Cl^- aqueous solution. The reason indicated by Makovos and Liu for the inactivity of gold in the presence of Cl^- is the dissolution of Au to $AuCl_4^-$ which prevents the formation of the oxide. However the Pourbaix diagram shows that above pH 9, gold is directly oxidized

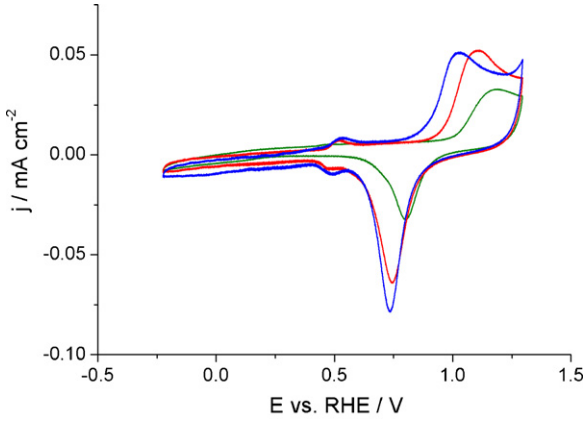

Fig. 3. Cyclic voltammetry at a gold pin electrode of 100 mM buffer (K_2HPO_4–KH_2PO_4) at different pH: 7.5 (green curve); 9.5 (red curve); 11.5 (blue curve). Scan rate 20 mV s^{-1}. (For interpretation of the references to colors in this figure legend, the reader is referred to the web version of this article.)

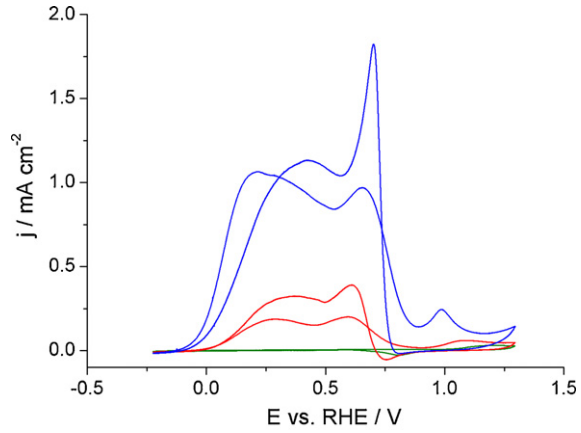

Fig. 4. Cyclic voltammetry at a gold pin electrode of 100 mM buffer (K_2HPO_4–KH_2PO_4) at different pH: 7.5 (green curve); 9.5 (red curve); 11.5 (blue curve) in the presence of glucose (10 mM). Scan rate 20 mV s^{-1}. (For interpretation of the references to colors in this figure legend, the reader is referred to the web version of this article.)

to $Au(OH)_3$ thus avoiding the formation of the tetrachloroaurate ion. This means that above pH 9, $Au(OH)_3$ should be formed, even in the presence of chlorides. To demonstrate this, CV measurements at pH 11.5 (buffered, 100 mM) in the presence of 10 mM glucose have been performed at different chloride concentrations (Fig. 6). As expected, in these conditions the chloride ions do not completely prevent the generation of peak (*), but the intensity of the peak does decrease as the concentration of Cl^- increases. The mechanism proposed by Makovos and Liu [25] cannot explain this phenomenon. We propose another mechanism: the chloride ions can strongly adsorb to the gold active sites thus inhibiting the oxidative adsorption of glucose, a key step in the overall oxidation process. To

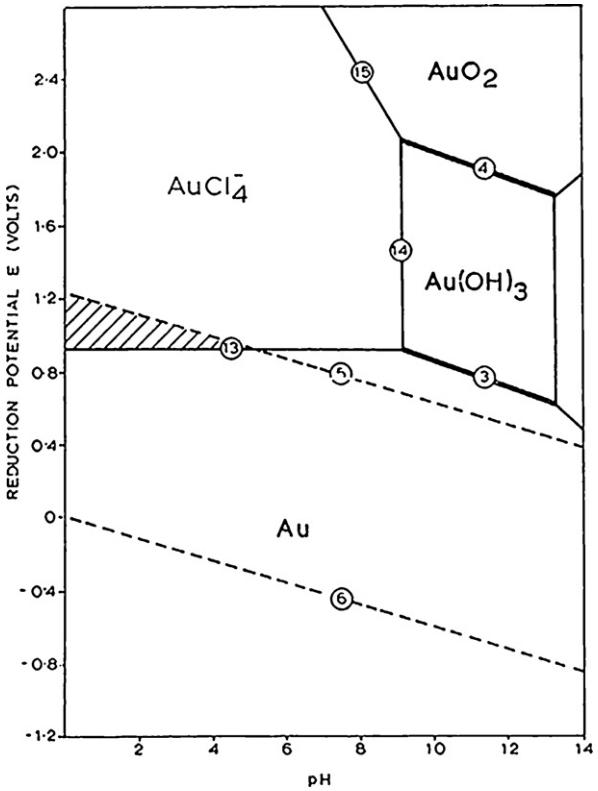

Fig. 5. Pourbaix diagram for the system Au–H_2O–Cl^- at 25 °C. $a = 10^{-2}$ M, $[Cl^-] = 2$ M, $pO_2 = pH_2 = 1$ atm. Extract from Ref. [30].

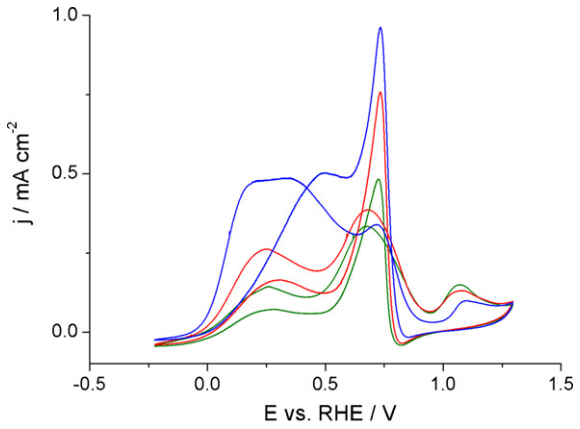

Fig. 6. Cyclic voltammetry at a gold pin electrode of 10 mM glucose in 100 mM buffer (K_2HPO_4–KH_2PO_4) at pH 11.5 and different chloride concentrations: (blue) without chloride ions, (red) 50 mM, (green) 100 mM. Scan rate 20 mV s^{-1}. (For interpretation of the references to colors in this figure legend, the reader is referred to the web version of this article.)

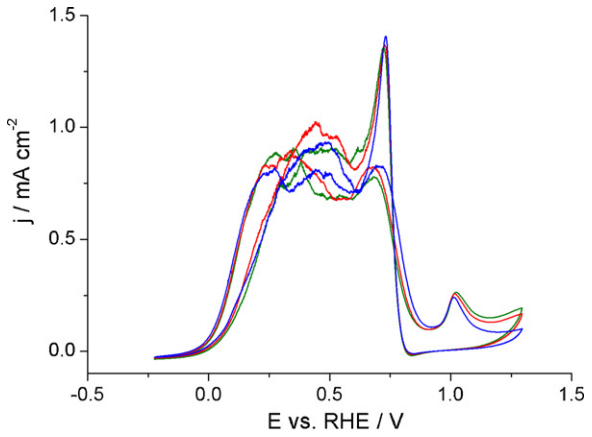

Fig. 8. Cyclic voltammetry at a gold pin electrode of 10 mM glucose in 100 mM buffer (K_2HPO_4–KH_2PO_4) at pH 11.5 and different fluoride concentrations: (red) without fluoride ions, (blue) 50 mM and (black) 100 mM. Scan rate 20 mV s^{-1}. (For interpretation of the references to colors in this figure legend, the reader is referred to the web version of this article.)

prove the adsorption of the chlorides to the surface, electrochemical impedance spectroscopy (EIS) techniques has been employed at fixed frequency and potential, while increasing the concentration of Cl^-. EIS at high frequency enables the gold/electrolyte interface to be studied. An adsorption of Cl^- to the surface should increase the differential capacitance; as a consequence the negative imaginary part of the impedance ($-Im(Z)$) should decrease. A preliminary EIS was performed in the range from 100 kHz to 100 mHz to establish the optimal working frequency (5 kHz). The experiment was performed recording the impedance every 10 s (Fig. 7). Obviously a decrease of the $Re(Z)$ is observed when increasing the KCl concentration, due to the increase of the conductivity. According to the results, after an initial period in which the value of $-Im(Z)$ slightly increases, it decreases for concentrations higher than 40 mM Cl^-.

The suspected importance of the adsorbed ions on the overall oxidation mechanism of glucose was confirmed by the replacement of Cl^- with F^-. It is expected that the interaction between a very hard ion, such as fluoride, with a soft element, like gold, is hindered, thus $-Im(Z)$ should remain constant in response to increasing fluoride concentration. The cyclic voltammograms after successive fluoride additions are reported in Fig. 8. As expected, the addition of fluorides does not affect the features of the cyclic voltammogram, meaning that the adsorption of F^- is negligible. This conclusion has been confirmed with the EIS measurement at fixed frequency and potential, while increasing the concentration of F^- (Fig. 9). In this case we can see a decrease of the $Re(Z)$, while the $-Im(Z)$ value is constant.

The very importance of the adsorbed species on the oxidation of the glucose gives rise to questions about the possible limitations generated by other species in solution, like the buffer. To address this question cyclic voltammetry of glucose oxidation was performed using only NaF (100 mM) as supporting electrolyte (Fig. 10). The presence of a very low buffer (KH_2PO_4\K_2HPO_4) concentration (1 mM) was necessary to obtain a reproducible cyclic voltammetry. The anodic limit was also shifted 150 mV toward more positive potentials with respect to the 100 mM buffer measurement to allow the $Au(OH)_3$ oxidation peak formation.

Interesting conclusions can be drawn by comparing Figs. 4 and 10. At pH 7.5 without buffer it is possible to observe the presence of the cathodic peak which is practically invisible with 100 mM buffer. This effect stresses that the buffer is also adsorbed on the active sites. The effect at higher pH is also very interesting. It is clearly visible that with fluoride as the supporting electrolyte the peak current density is about 5 times lower. This can be easily explained by considering the real purpose of the buffer: to maintain a constant pH near the gold surface [10]. This process is very slow when only

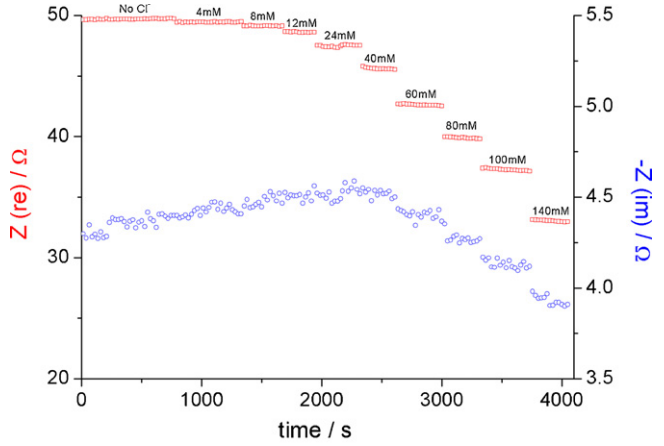

Fig. 7. Continuous EIS measurement at 5 kHz of Au pin electrode in 100 mM K_2HPO_4, pH 11.5 with increasing chloride concentration. $Re(Z)$ in red squares and $-Im(Z)$ in blue circles. (For interpretation of the references to colors in this figure legend, the reader is referred to the web version of this article.)

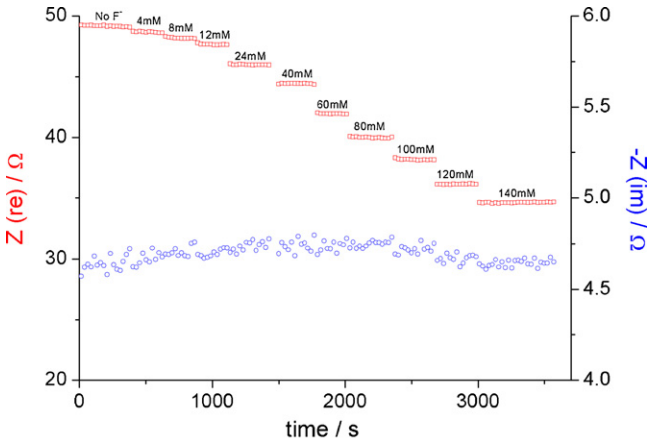

Fig. 9. Continuous EIS measurement at 5 kHz of Au pin electrode in 100 mM K_2HPO_4, at pH 11.5 with increasing fluoride concentration. $Re(Z)$ in red squares and $-Im(Z)$ in blue circles. (For interpretation of the references to colors in this figure legend, the reader is referred to the web version of this article.)

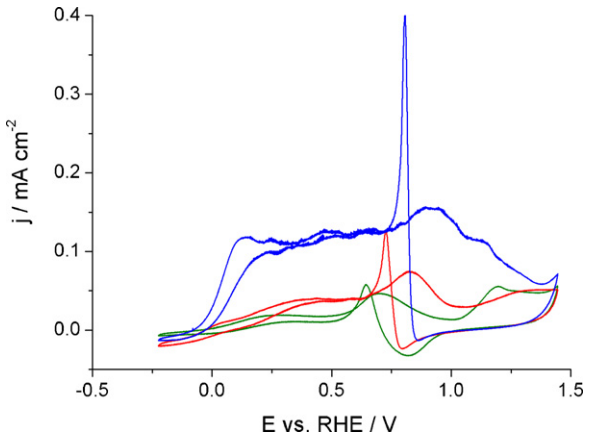

Fig. 10. Cyclic voltammetry at a gold pin electrode of 100 mM NaF, 1 mM (K_2HPO_4–KH_2PO_4) at different pH: 7.5 (green); 9.5 (red); 11.5 (blue) in the presence of glucose (10 mM). Scan rate 20 mV s^{-1}.

fluoride ions are present, being OH^- ions provided only through transport. So the buffer has two contrasting effects: it adsorbs to the surface, decreasing the active sites for the oxidation of glucose and it also keeps constant the pH at the surface of the gold electrode. This second effect is predominant at high pH values.

On the basis of the experimental data and considerations reported in this section, a mechanism of the generation of the oxidative peak (*) is proposed in the next section.

3.1. Model of glucose oxidation

Here the electrochemical oxidation of glucose to gluconate is analyzed in mechanistic detail. The aim is to understand the origin of the oxidative peak in the reductive sweep of the cyclic voltammetry, a peculiar feature already studied for its implication in glucose sensing [25]. The mechanism proposed is based on previous studies on platinum [10] and gold [24] electrodes. Fig. 11 summarizes the mechanism and the main species involved. At first, the glucose molecule is electrochemically adsorbed at the surface of the electrode by dehydrogenation (reaction (1)). The dehydrogenated molecule can be transformed to gluconate by direct oxidation (reac-

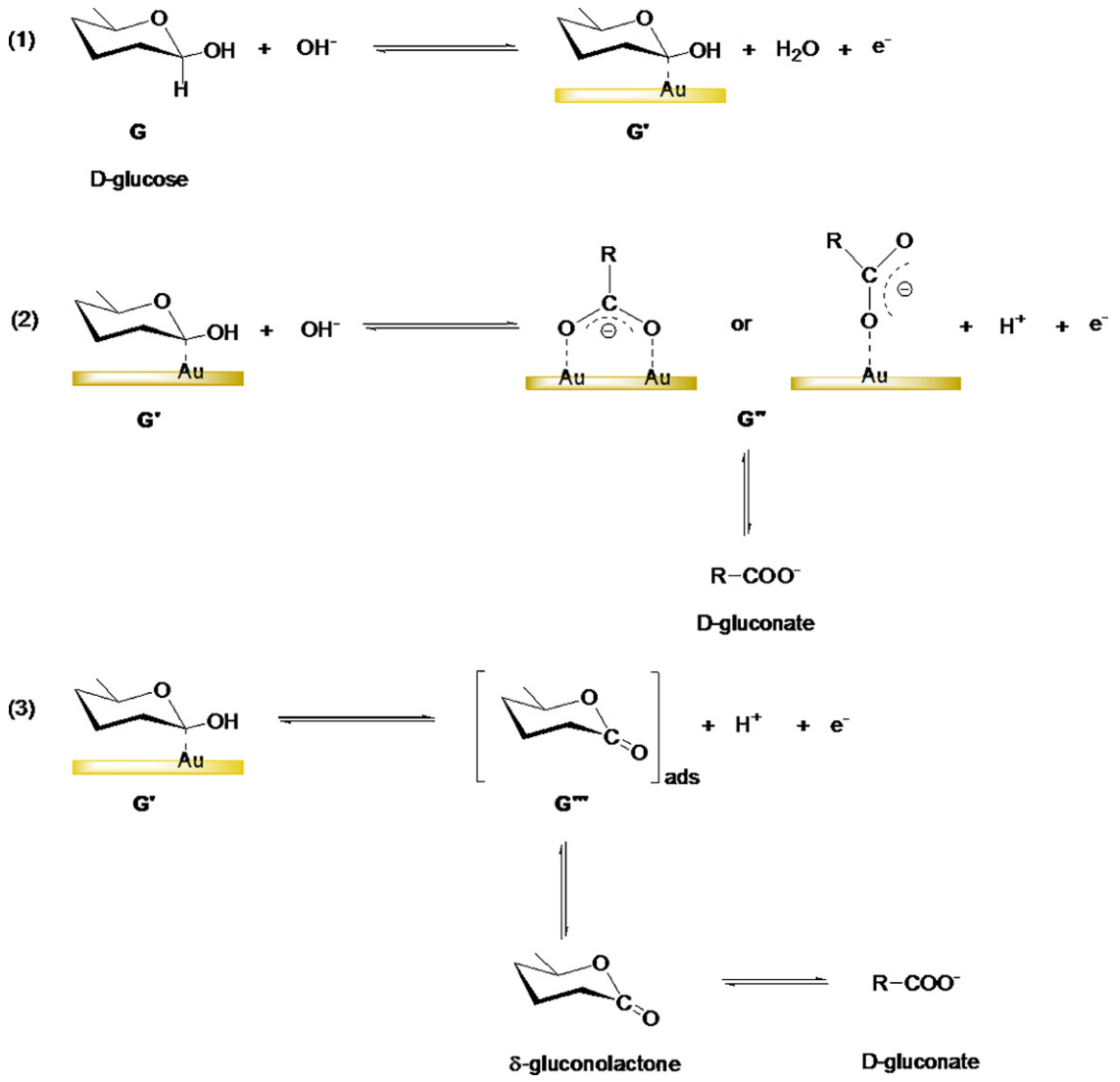

Fig. 11. Proposed mechanism at gold electrodes. G = D-glucose (β-D-glucopyranose formed predominantly in water), G′ = dehydrogenated glucose (intermediate generated by anomeric carbon dehydrogenation), G″ = D-gluconate, G‴ = δ-gluconolactone.

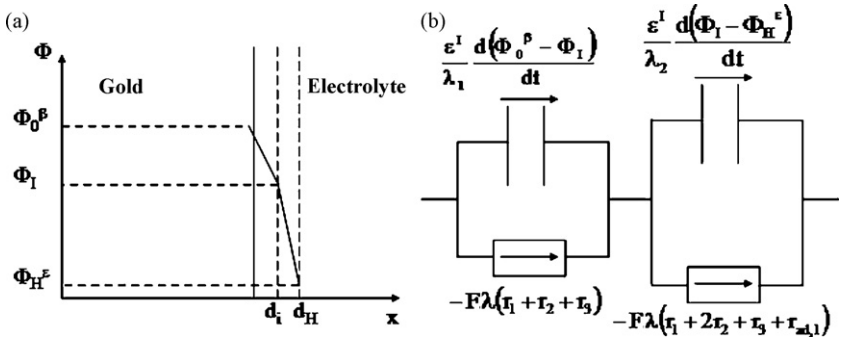

Fig. 12. (a) Potential distribution at the solid phase/electrolyte interface. (b) Current flow through the gold/electrolyte interface.

Table 1
Summary of fixed simulation parameters.

$k_{1,k,o}$	$k_{1,a,o}$	$k_{2,k,o} + k_{3,k,o}$	$k_{2,o,o}/k_{2,k,o}$	$k_{3,o,o}/k_{3,k,o}$
10^{-10}	10^{-7}	8×10^{-1}	1	1
$k_{ad,1,k,o}$	$k_{ad,2,k,o}$	N_I/mol cm^{-3}	λ/cm	λ_2/cm
10^{-7}	8×10^{-3}	10^{-1}	4×10^{-3}	2×10^{-3}

tion (2)), which involves the production of a hydroxide ion and the elimination of an H^+. An alternative path is the oxidization of the dehydrogenated glucose to δ-gluconolactone (reaction (3)). The δ-gluconolactone is then transformed to gluconate after reacting with a hydroxide ion.

$$G'_{(I)} + H_2O_{(\varepsilon)} + e^-_{(\beta)} \underset{k_{1,O}}{\overset{k_{1,R}}{\rightleftarrows}} G_{(\varepsilon)} + OH^-_{(\varepsilon)} \quad (1)$$

$$G''^-_{(I)} + H^+_{(\varepsilon)} + e^-_{(\beta)} \underset{k_{2,O}}{\overset{k_{2,R}}{\rightleftarrows}} G'_{(I)} + OH^-_{(\varepsilon)} \quad (2)$$

$$G'''_{(I)} + H^+_{(\varepsilon)} + e^-_{(\beta)} \underset{k_{3,O}}{\overset{k_{3,R}}{\rightleftarrows}} G'_{(I)} \quad (3)$$

Here the subscript I indicates the inner Helmholtz layer of the interface, ε the solution and β the electrode. The electrochemical reactions are written following the electrochemical convention of reduction as the direct reaction and oxidation as the inverse one. The molecules represented by the symbols G, G′, G″, and G‴ are reported in Fig. 11, and are glucose, dehydrogenated glucose, gluconate, and δ-gluconolactone, respectively. Our electrochemical experiments confirm that the oxidation of glucose is blocked at the surface of the gold hydroxide, as previously pointed out by Xiang et al. [28]. We described the reaction rates for the ith reaction, r_i, as:

$$r_1 = k_{1,R} N_I \gamma' - k_{1,O} a_G^\varepsilon a_{OH}^\varepsilon (1 - \gamma' - \gamma'' - \gamma''')(a_{Au})^m$$
$$r_2 = k_{2,R} N_I \gamma'' a_H^\varepsilon - k_{2,O} N_I \gamma' a_{OH}^\varepsilon \quad (4)$$
$$r_3 = k_{3,R} N_I \gamma''' a_H^\varepsilon - k_{3,O} N_I \gamma'$$

where N_I is the number of sites available in the inner Helmholtz layer, γ', γ'', γ''' are the fraction of sites occupied by the dehydrogenated glucose, gluconate and δ-gluconolactone, respectively, a_G^ε is the activity of glucose molecules in the electrolyte, a_{OH}^ε the activity of hydroxide ions in the electrolyte, a_H^ε the activity of protons in the electrolyte, and a_{Au} the activity of gold at the surface of the gold electrode. The exponent m of a_{Au} is dependent on the number of gold atoms necessary to coordinate the oxidation of the glucose. Empirically, it should be greater than 1. The kinetic constants of the electrochemical reactions (1)–(3) are dependent on the electric potential distribution at the interface:

$$\frac{k_{1,R}}{k_{1,R,0}} = \exp\left[-\frac{F\left(\Phi_0{}^\beta - \Phi_H{}^\varepsilon\right)}{2RT}\right], \quad \frac{k_{1,O}}{k_{1,O,0}} = \exp\left[\frac{F\left(\Phi_0{}^\beta - \Phi_H{}^\varepsilon\right)}{2RT}\right]$$
$$\frac{k_{2,R}}{k_{2,R,0}} = \exp\left[-\frac{F\left(\Phi_0{}^\beta + \Phi_I - 2\Phi_H{}^\varepsilon\right)}{2RT}\right], \quad \frac{k_{2,O}}{k_{2,O,0}} = \exp\left[\frac{F\left(\Phi_0{}^\beta + \Phi_I - 2\Phi_H{}^\varepsilon\right)}{2RT}\right] \quad (5)$$
$$\frac{k_{3,R}}{k_{3,R,0}} = \exp\left[-\frac{F\left(\Phi_0{}^\beta - \Phi_H{}^\varepsilon\right)}{2RT}\right], \quad \frac{k_{3,O}}{k_{3,O,0}} = \exp\left[\frac{F\left(\Phi_0{}^\beta - \Phi_H{}^\varepsilon\right)}{2RT}\right]$$

where F is the Faraday constant, R the universal gas constant, T the absolute temperature, ϕ_0^β the electric potential at the surface

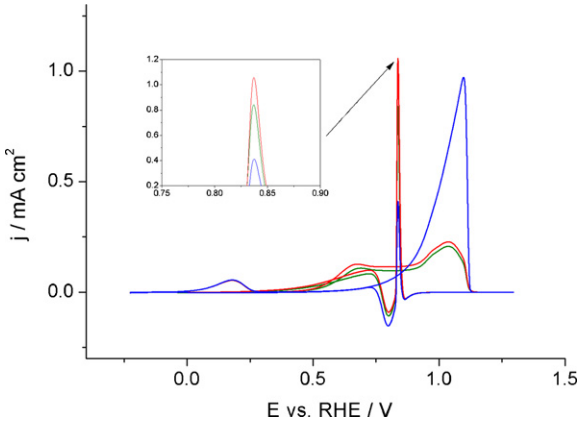

Fig. 13. Simulation of the electrochemical oxidation of glucose. No adsorption of other species considered. Parameters are in Table 1. Green $r = 1$, red $r = 0$, blue $r = \infty$. (For interpretation of the references to colors in this figure legend, the reader is referred to the web version of this article.)

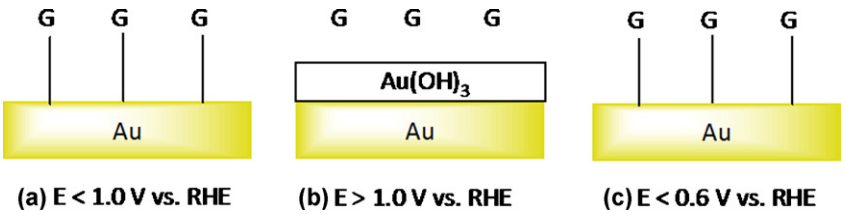

Fig. 14. Schematic of the formation of the oxidative peak in the cathodic scan. (a) As long as the potential of the electrode is below 1.05 V vs. RHE glucose can adsorb to the gold surface, first step of the oxidation reaction. (b) At potential higher than 1.05 V vs. RHE gold surface is oxidized to gold hydroxide, inactive toward glucose electro-oxidation (c) during the cathodic scan gold is reduced at potentials around 0.6 V vs. RHE, glucose can adsorb again and get oxidized, generating the oxidative peak in the cathodic scan. The different in potential for gold hydroxide formation and reduction is due to overpotential.

of the gold electrode, ϕ_H^{ε} the electric potential of the solution at the Helmholtz plane (d_H in Fig. 12), and Φ_I the electric potential in the inner Helmholtz layer. The electric field in the inner Helmholtz layer is not constant, due to the presence of the gluconate, which is a charged species (see Fig. 12). In Fig. 12 the current flow through the electrode is reported. The correlation between the fraction of the occupied sites of the different compounds and the reaction rates is given by:

$$\begin{aligned}\lambda N_I \frac{d\gamma'}{dt} &= -\lambda r_1 + \lambda r_2 + \lambda r_3 \\ \lambda N_I \frac{d\gamma''}{dt} &= -\lambda r_2 - \lambda r_{ad,1} \\ \lambda N_I \frac{d\gamma'''}{dt} &= -\lambda r_3 - \lambda r_{ad,2}\end{aligned} \tag{6}$$

where λ is the distance between the surface of the electrode and the Helmholtz plane, and $r_{ad,1}$ and $r_{ad,2}$ are the reaction rates of the desorption of the gluconate and the δ-gluconolactone, respectively. The desorption reaction rates can be expressed by:

$$\begin{aligned}r_{ad,1} &= k_{ad,1,R} N_I \gamma'' - k_{ad,1,O} a_{G''}{}^{\varepsilon} (1 - \gamma' - \gamma'' - \gamma''')(a_{Au})^m \\ r_{ad,2} &= k_{ad,2,R} N_I \gamma''' - k_{ad,2,O} a_{G'''}{}^{\varepsilon} (1 - \gamma' - \gamma'' - \gamma''')(a_{Au})^m\end{aligned} \tag{7}$$

with the kinetic parameters equal to:

$$\frac{k_{ad,1,R}}{k_{ad,1,R,0}} = \exp\left[-\frac{F(\Phi_I - \Phi_H{}^{\varepsilon})}{2RT}\right], \quad \frac{k_{ad,1,O}}{k_{ad,1,O,0}} = \exp\left[\frac{F(\Phi_I - \Phi_H{}^{\varepsilon})}{2RT}\right]$$
$$\frac{k_{ad,2,R}}{k_{ad,2,R,0}} = 1, \qquad \frac{k_{ad,2,O}}{k_{ad,2,O,0}} = 1 \tag{8}$$

We want to stress that the reaction of desorption of gluconate involves charged species, therefore passage of reductive current, as reported in Fig. 12. On the other hand, desorption of δ-gluconolactone does not involve passage of charged species.

To prove that the proposed mechanism can justify the presence of the oxidative peak (*), simulations of the oxidation of glucose were made using a program compiled with MATLAB 7.0. From an intuitive point of view, when the activity of gold at the surface decreases (due to the formation of gold hydroxide), the reaction rates r_1, r_2, and r_3 slow down, while reaction $r_{ad,1}$ and $r_{ad,2}$ become more positive. The result is a decrease of the adsorbed species. When the oxide is reduced, the naked gold surface is ready to oxidize the glucose. We will demonstrate that the ratio of the reaction rates of the two alternative mechanisms of formation of the gluconate (reactions (2) and (3)) is relevant in observing the oxidative peak (*) (see Fig. 1). The simulations do not include transport phenomena, nor the activity coefficients of the species, therefore it is not expected to completely reproduce the experimental cyclic voltammetry curve. Nevertheless, the main features (number of peaks and the peak (*)) should be reproduced.

The fixed parameters of the simulations are given in Table 1. The parameter r is the ratio between $k_{d,2}$ and $k_{d,3}$. In Fig. 13 the simulations for different values of r are reported. Absorption of other ions except glucose is neglected (like in the fluorides). The simulations should be compared with Fig. 10. The effect of the parameter r on reaction (1) is negligible, while it is very important in the shape of the cyclic voltammetry curve above 0.3 V vs. RHE. When $r = \infty$, most of the dehydrogenated glucose is oxidized to δ-gluconolactone near 0.6 V vs. RHE. The desorption of δ-gluconolactone does not involve current flow; a limiting current is reached. After the formation of gold hydroxide (at 1.05 V vs. RHE) the oxidation of glucose stops, and the surface desorbs all the adsorbed species. Decreasing the potential, the reduction of gold hydroxide generates new gold surface, active to the oxidation of glucose (Fig. 14). The peak (*) is observed in the simulations. Its intensity is much higher than in experimental data, due to the fact that diffusion has not been considered. Under these conditions, the limiting reactant is the number of active sites at the gold surface, which is immediately saturated. By decreasing the value of r, the intensity of the peak (*) decreases. This is an effect of the gluconate. The gluconate is a negatively charged species and therefore is attracted to the surface of the electrode at high voltages. When the potential of the electrode is increased, the gluconate desorbs much more slowly than the δ-gluconolactone, therefore less active sites are available when the glucose oxidation starts again.

Fig. 15 shows the simulated results of the effect of adsorption on the peak (*). The figure reports two curves, simulating the presence of F^- (no adsorption) and Cl^- (chemisorption) respectively. As expected from the experimental data, the presence of Cl^- partially blocks the active sites, thus decreasing the intensity of the peak (*). We want to stress that in the case of Cl^- adsorption, the reaction rate for each step in the oxidation of glucose decreases, as observed in the experimental section (see Fig. 6). The simulations support the mechanism we have proposed for the generation of the peak (*) and the influence of the other species in the electrolyte on its intensity.

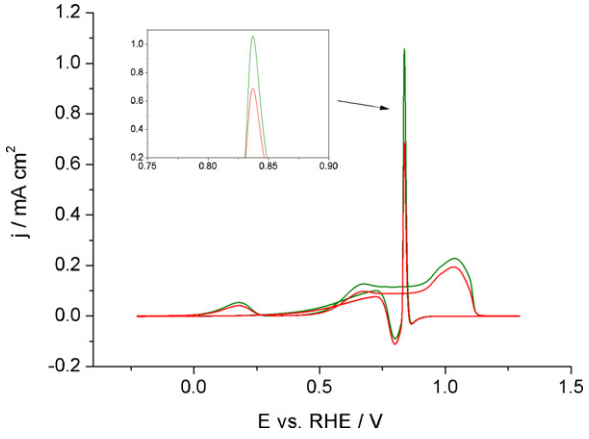

Fig. 15. Simulation of the electrochemical oxidation of glucose, with $r = 0$. Green no adsorption, red adsorption (100 mM). (For interpretation of the references to colors in this figure legend, the reader is referred to the web version of this article.)

4. Conclusions

This paper has proposed a mechanism to explain the oxidation peak in the cathodic scan at gold electrodes in which the key step is the competitive adsorption at the active sites of the ionic species present in the solution (phosphate buffer, chlorides and OH^-) and the substrate (glucose). Simulations of the proposed mechanism have supported the plausibility of the mechanism. The study represents the basis for upcoming work on glucose sensing at gold electrodes.

Acknowledgements

Y.C. acknowledges support from the King Abdullah University of Science and Technology (KAUST) Investigator Award (No. KUS-I1-001-12). The authors wish to thank Heather Deshazer for her help in preparing the manuscript.

References

[1] S. Kerzenmacher, F J., R. Zengerle, F. von Stetten, J. Power Sources 182 (2008) 1.
[2] A. Heller, B. Feldman, Chem. Rev. (Washington, DC, US), 108 (2008) 2482.
[3] J.M. Ekoé, The Epidemiology of Diabetes Mellitus, Wiley-Blackwell/Hoboken, Chichester, UK/NJ, 2008.
[4] M. Tominaga, M. Nagashima, K. Nishiyama, I. Taniguchi, Electrochem. Commun. 9 (2007) 1892.
[5] I.T. Bae, E. Yeager, X. Xiang, C.C. Liu, J. Electroanal. Chem. Interfacial Electrochem. 309 (1991) 131.
[6] S. Ben Aoun, I. Taniguchi, Chem. Lett. 37 (2008) 936.
[7] L.H.E. Yei, B. Beden, C. Lamy, J. Electroanal. Chem. Interfacial Electrochem. 246 (1988) 349.
[8] N.N. Nikolaeva, O.A. Khazova, Y.B. Vasil'ev, Elektrokhimiya 19 (1983) 1476.
[9] N.N. Nikolaeva, O.A. Khazova, Y.B. Vasil'ev, Elektrokhimiya 16 (1980) 1227.
[10] B. Beden, F. Largeaud, K.B. Kokoh, C. Lamy, Electrochim. Acta 41 (1996) 701.
[11] J.R. Rao, G.J. Richter, F. Von Sturm, E. Weidlich, Bioelectrochem. Bioenerg. 3 (1976) 139.
[12] U. Gebhardt, G. Luft, G.J. Richter, F. Von Sturm, Bioelectrochem. Bioenerg. 5 (1978) 607.
[13] M. Tominaga, T. Shimazoe, M. Nagashima, H. Kusuda, A. Kubo, Y. Kuwahara, I. Taniguchi, J. Electroanal. Chem. 590 (2006) 37.
[14] M. Tominaga, T. Shimazoe, M. Nagashima, I. Taniguchi, Electrochem. Commun. 7 (2005) 189.
[15] Y.-G. Zhou, S. Yang, Q.-Y. Qian, X.-H. Xia, Electrochem. Commun. 11 (2009) 216.
[16] Y. Bai, W. Yang, Y. Sun, C. Sun, Sens. Actuators B B134 (2008) 471.
[17] J.-J. Yu, S. Lu, J.-W. Li, F.-Q. Zhao, B.-Z. Zeng, J. Solid State Electrochem. 11 (2007) 1211.
[18] C. Jin, I. Taniguchi, Chem. Eng. Technol. 30 (2007) 1298.
[19] B.K. Jena, C.R. Raj, Chem. Eur. J. 12 (2006) 2702.
[20] M. Tominaga, T. Shimazoe, M. Nagashima, I. Taniguchi, Chem. Lett. 34 (2005) 202.
[21] M.W. Hsiao, R.R. Adzic, E.G. Yeager, J. Electrochem. Soc. 143 (1996) 759.
[22] K.B. Kokoh, J.M. Leger, B. Beden, H. Huser, C. Lamy, Electrochim. Acta 37 (1992) 1909.
[23] R.R. Adzic, M.W. Hsiao, E.B. Yeager, J. Electroanal. Chem. Interfacial Electrochem. 260 (1989) 475.
[24] N.N. Nikolaeva, O.A. Khazova, Y.B. Vasil'ev, Elektrokhimiya 19 (1983) 1042.
[25] E.B. Makovos, C.C. Liu, Bioelectrochem. Bioenerg. 15 (1986) 157.
[26] W.R. LaCourse, D.C. Johnson, Anal. Chem. 65 (1993) 50.
[27] D.W. Kirk, F.R. Foulkes, W.F. Graydon, J. Electrochem. Soc. 127 (1980) 1069.
[28] C. Xiang, Q. Xie, S. Yao, Electroanalysis 15 (2003) 987.
[29] M.J. Nicol, Gold Bull. 13 (1980) 105.
[30] N.P. Finkelstein, R.D. Hancock, Gold Bull. 7 (1974) 72.